Muon spin relaxation study of the stripe phase order in $La_{1.6-x}Nd_{0.4}Sr_xCuO_4$ and related 214 cuprates

B. Nachumi, Y. Fudamoto, A. Keren,* K. M. Kojima,† M. Larkin,
G. M. Luke, J. Merrin, O. Tchernyshyov, and Y. J. Uemura
Physics Department, Columbia University, New York, New York 10027

N. Ichikawa, M. Goto, H. Takagi, and S. Uchida
Department of Superconductivity, University of Tokyo, Bunkyo-ku, Tokyo 113, Japan

M. K. Crawford and E. M. McCarron
DuPont, Wilmington, Delaware 19880-0356

D. E. MacLaughlin
Department of Physics, University of California, Riverside, California 92521

R. H. Heffner
MS K764, Los Alamos National Laboratory, Los Alamos, New Mexico 87545

(Received 23 April 1998)

We present zero-field muon spin relaxation (μSR) measurements of $La_{1.6-x}Nd_{0.4}Sr_xCuO_4$ with $x=0.125,0.15,0.2$; $La_{1.475}Nd_{0.4}Ba_{0.125}CuO_4$, $La_{1.875}Ba_{0.125}CuO_4$, and $La_{1.875}Ba_{0.125-y}Sr_yCuO_4$ with $y=0.025,0.065$. All of the samples with dopant concentrations $x+y\leqslant 0.15$ show similar static magnetic order with coherent precession of the muon spins below $T_N\approx 30$ K, with a $T\rightarrow 0$ ordered Cu moment $\approx 0.3\mu_B$. The samples with $x=0.20$ show no coherent precession but manifest two distinct relaxation regimes, typical of quasistatic magnetism. We then present transverse-field μSR hysteresis measurements of the $La_{1.45}Nd_{0.4}Sr_{0.15}CuO_4$ and $La_{1.4}Nd_{0.4}Sr_{0.2}CuO_4$ systems that show a large superconducting response below approximately 7 K and 12 K, respectively. We argue that superconductivity and magnetic order coexist in the $x=0.15$ system. [S0163-1829(98)09837-3]

I. INTRODUCTION

There is a complex interplay between superconductivity and antiferromagnetism as a function of doping in the ''214'' high-T_c cuprate superconductors $La_{2-x}Sr_xCuO_4$ and $La_{2-x}Ba_xCuO_4$. The phase diagram for these materials as a function of temperature and doping is reproduced in Figs. 1 and 2. As with all the cuprates, the undoped parent material is an antiferromagnet, with a transition temperature $T_N\approx 300$ K. With increasing x, the antiferromagnetic (AF) order is destroyed; both $La_{2-x}Ba_xCuO_4$ and $La_{2-x}Sr_xCuO_4$ move through a spin-glass-like disordered phase (SG) and eventually become superconducting at dopant concentrations of 0.05 and 0.07, respectively. However, at $x\approx 0.125$ in $La_{2-x}Ba_xCuO_4$ and $x\approx 0.115$ in $La_{2-x}Sr_xCuO_4$, superconductivity is suppressed and magnetic order reemerges—the phenomenon known as the ''1/8 effect.''[1–4]

Descriptions of these materials from the AF and superconductor (SC) sides of the phase diagram have recently concentrated on the importance of ''stripe correlations'' between nearly one-dimensional strips of the CuO_2 plane. Borsa *et al.*[5] have described the low-temperature magnetization for doped AF, $x<0.02$ samples with a phenomenological spin-wave model where the magnetic domains are finite in one planar direction and bounded by segregated ''charge rivers.'' Hone and Castro Neto[6] have treated the weak AF stripe problem more generally within a nonlinear σ model, and have reproduced the observed dependence of the magnetic transition temperature on the extrapolated $T\rightarrow 0$ magnetization. On the SC side, neutron-scattering studies have consistently revealed low-energy dynamics[7–9] that appear as satellite peaks near the AF Bragg peak $(\pi/a,\pi/a)$ in SC samples of $La_{2-x}Sr_xCuO_4$, with a splitting wave vector of magnitude $\epsilon\sim x\times 2\pi/a$ where a is the Cu-O-Cu lattice spacing in the plane.

A stripe mechanism has been proposed to explain the ''1/8 effect'' as the pinning of the dynamic stripe correlations on distortions in the CuO_2 plane.[10,11] The structural transitions of $La_{1.875}Ba_{0.125}CuO_4$ are shown in Fig. 1. Successive transitions in $La_{1.875}Ba_{0.125}CuO_4$ from high-temperature tetragonal (HTT) to orthorhombic (LTO) to low-temperature tetragonal (LTT) structural phases involve successive distortions or rotations of the CuO_6 octahedra. From the HTT phase, the octahedra distort about the tetragonal (110) axis, diagonally furrowing the CuO_2 plane. In the LTO→LTT transition, the octahedra distort about the twinned $(1\overline{1}0)$ axis. The superposition of these two distortions tends to buckle the CuO_2 plane in the (100) and (010) directions of successive CuO_2 layers. X-ray measurements[1] show that in $La_{1.875}Ba_{0.125}CuO_4$, the LTO and LTT phases coexist well below the onset of the structural transition; the suppression of superconductivity roughly correlates with the fraction of the sample in the LTT phase at low temperature.

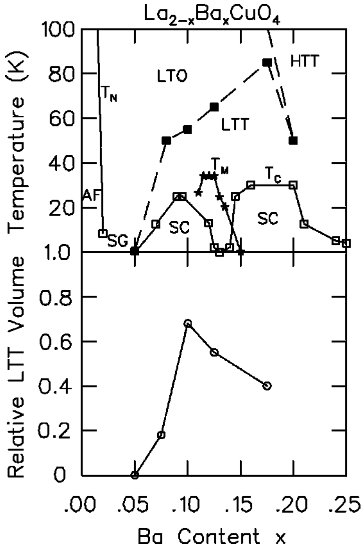

FIG. 1. Electronic and structural phase diagrams as a function of temperature and doping x for $La_{2-x}Ba_xCuO_4$ (Refs. 1–3). The electronic phases are indicated by solid lines connecting the open squares. The electronic phases are antiferromagnetic (AF) and superconductor (SC). The structural phases are indicated by dotted lines connecting the filled squares.

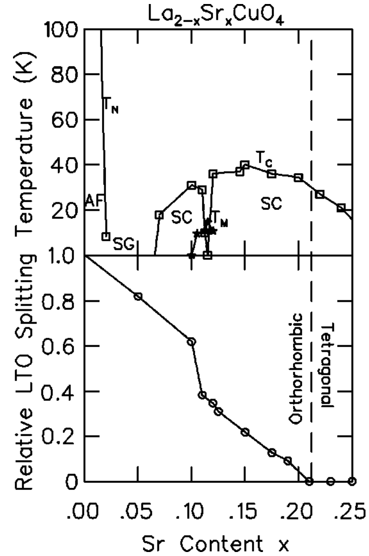

FIG. 2. Electronic and structural phases as a function of temperature and doping x for $La_{2-x}Sr_xCuO_4$ (Refs. 3, 5, and 12).

In $La_{2-x}Sr_xCuO_4$,[12] by contrast, only the HTT and LTO phases are stable. The superconductivity in this compound is correspondingly more robust. In the $La_{1.6-x}Nd_{0.4}Sr_xCuO_4$ system the LTT phase is stabilized over a wide doping range with very little orthorhombic contamination below the transition, as shown in the phase diagram of Fig. 3.[13–15] Büchner *et al.*[15] have argued that superconductivity is suppressed for LTT phases of $La_{1.6-x}Nd_{0.4}Sr_xCuO_4$ in which the tilting of the octahedra exceeds a critical angle of 3.6°, i.e., for Nd concentrations >0.18 per formula unit.

On the hypothesis that the planar distortions associated with the LTO→LTT transition would pin dynamic magnetic correlations seen in superconducting samples of $La_{2-x}Sr_xCuO_4$, and motivated by the appearance of a stripe-charge-segregation/magnetic order in the analogous nickelate perovskite,[16] Tranquada *et al.*[10,11] searched for and found static magnetic order for $x=0.125,0.15,0.2$ in $La_{1.6-x}Nd_{0.4}Sr_xCuO_4$ using neutron-scattering techniques. In the $x=0.125$ sample, Tranquada *et al.* found a charge segregation that preceded the magnetic order. Below the LTO→LTT transition, at T_{CO}, the charge segregated into striped domains parallel to the distortions in the CuO_2 plane.[1,17] At $T_M<T_{CO}$, a locally AF order arose within the regions presumably bounded by the charge stripes, with neighboring AF regions out of phase by π.

Recent superconducting quantum interference device (SQUID) measurements[18] suggest that superconductivity and stripe magnetic order coexist in these materials, which raises the interesting possibility of the existence of a superconducting network of quasi-one-dimensional wires (the charge-rich stripes). However, there has been no confirmation of the relative magnetic and superconducting volume fractions in a single sample.

μSR techniques have been instrumental in establishing the magnetic phase diagrams of the doped La_2CuO_4 systems. The homogeneous AF phase of La_2CuO_{4-y} with $T_N \approx 290$ K was first seen with μSR by Uemura *et al.*[19] Subsequent studies on La_2CuO_{4-y} with $0<y<0.03$ showed that, although T_N varied substantially with y, the magnetization remained approximately constant.[20] Harshman *et al.* first identified the SG phase with μSR.[21] Hitti *et al.*[22] identified the muon site in La_2CuO_{4-y} by comparing neutron-scattering measurements of the moment size to the μSR precession frequency. As already mentioned, the lightly Sr-doped region has been explored by Borsa *et al.*

The magnetism associated with the ''1/8 effect'' was first identified in $La_{1.875}Ba_{0.125}CuO_4$ by Luke *et al.*,[2] and for $La_{1.885}Sr_{0.115}CuO_4$, by Kumagai *et al.*[3] In the wake of the neutron-scattering studies of Tranquada *et al.*, four groups reported new μSR measurements on variously doped La_2CuO_4 systems. Wagener *et al.* presented a study of $La_{1.85-z}Nd_zCuO_4$ that confirmed the presence of magnetic order for $z>0.3$.[23] Lappas *et al.* found that a suppression of the LTO→LTT transition by substitution of Sr for Ba in $La_{1.875}Ba_{0.125}CuO_4$, or by the addition of excess oxygen, destabilized the ''1/8 effect'' in this material.[24] Lappas *et al.* and Luke *et al.*[4] confirmed with μSR the magnetic order seen in $La_{1.475}Nd_{0.4}Sr_{0.125}CuO_4$, and compared the μSR frequencies in the systems with and without Nd.

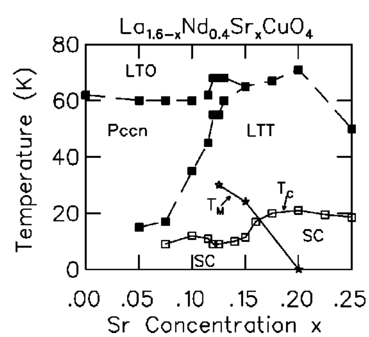

FIG. 3. Structural and electronic phase diagram for $La_{1.6-x}Nd_{0.4}Sr_xCuO_4$ (Refs. 11 and 13–15).

In this paper, we present a more detailed analysis of the data in Refs. 2 and 4, along with previously unpublished μSR data from $La_{1.875}Ba_{0.125-x}Sr_xCuO_4$, $La_{1.45}Nd_{0.4}Sr_{0.15}CuO_4$, and $La_{1.4}Nd_{0.4}Sr_{0.2}CuO_4$ systems. The present study has two purposes. First, using the techniques of zero-field (ZF) μSR, we investigate the nature of the magnetic order in a large variety of Ba-doped ''1/8'' and Sr-doped samples that contain Nd. We extract the magnetic ordering temperature T_N, and the ordered Cu moment S_0. The behavior of the Cu spins in all of these compounds is almost certainly the same, the only differences being due to secondary ordering of the Nd moments. In terms of the ratio of the ordered moment to the scaled transition temperature T_N/J_{AF}, where J_{AF} is the largest coupling constant in the system, previous μSR studies[25] have established the different qualitative behaviors of quasi-two-dimensional systems of $S=1/2$ ions (like the cuprate antiferromagnets) and quasi-one-dimensional systems (like the $S=1/2$ spin chain compounds and the 3-leg ''ladder'' cuprate). We compare the stripe materials to previously measured low-dimensional cuprate antiferromagnets.

Second, we demonstrate that in $La_{1.45}Nd_{0.4}Sr_{0.15}CuO_4$ magnetism and superconductivity coexist in the same sample volume. Using the techniques of transverse-field (TF) μSR, we show that single crystals of $La_{1.45}Nd_{0.4}Sr_{0.15}CuO_4$ and $La_{1.4}Nd_{0.4}Sr_{0.2}CuO_4$ show similarly large hysteresis effects attributable to flux pinning in the superconducting state. The $La_{1.45}Nd_{0.4}Sr_{0.15}CuO_4$ crystal was then pulverized. ZF-μSR measurements on this powdered sample show that the *entire sample* becomes magnetic. This suggests that the superconducting and magnetic phases microscopically coexist in the stripe phase.

II. ZF-μSR METHOD

In time-differential μSR, 100% polarized muons are implanted, one at a time into a sample. The muon generally resides in a well-defined location in the unit cell of the lattice, and precesses about the local magnetic field $\vec{B}_{\rm local}$ until it decays into a positron and two neutrinos. The positron is preferentially emitted along the instantaneous direction of the muon spin. One statistically reconstructs the muon polarization as a function of time by forming the asymmetry between the numbers of positrons emitted parallel and antiparallel to the original muon polarization direction $\hat{P}_\mu$.

The number of positron counts through each detector is histogrammed as a function of time. The histograms have the general form $N(t)=N_0e^{-t/\tau_\mu}[1+CIG(t)]$. Here N_0 is the total number of decay positrons in the histogram that would be seen in the absence of any initial polarization. N_0 is proportional to the total number of muons stopped, to the averaged energy acceptance of each detector, and to the solid angle of each detector. τ_μ is the lifetime of a muon at rest, approximately 2.197 μs. C is the projection of $\hat{P}_\mu$ onto the line connecting the center of the sample with the center of the detector and is equal to ± 1 for ZF measurements. I is the intrinsic asymmetry of the muon counter. This is the asymmetry of the muon decay as a function of energy, averaged over the energy acceptance and solid angle of the detector. For detectors of identical construction, placed symmetrically with respect to the sample, I will not change from detector to detector. Even when this is not the case, the distortions due to the differing intrinsic asymmetries is usually small.

The normalized polarization function, $G(t)$, contains all of the information related to the magnetic field in the sample. In what follows, I is assumed to be constant (that is, the detectors are identical). The quantity

$$\frac{N_+(t)-N_-(t)}{N_+(t)+N_-(t)}$$

defines the experimental asymmetry $A_{\rm exp}(t)$. If we normalize by the N_0 for one of the detectors, then we may write

$$A_{\rm exp}(t)=\frac{1-\alpha+(1+\alpha)IG(t)}{1+\alpha+(1-\alpha)IG(t)},$$

where $\alpha=N_{0,+}/N_{0,-}$. We invert the expression for $A_{\rm exp}(t)$ to obtain the ''corrected asymmetry'' $A(t)$, where

$$A(t)=IG(t)=\frac{A_{\rm exp}(t)(1+\alpha)+\alpha-1}{1+\alpha+A_{\rm exp}(t)(\alpha-1)}.$$

We now outline the general features of the ZF-μSR corrected asymmetry spectrum. If a well-defined electronic spin structure exists, then muon spins implanted at magnetically equivalent lattice sites precess in identical fashion, leading to a statistically large precession of the muon spin asymmetry signal at a frequency defined by the field at that site: $\nu=\gamma_\mu/2\pi B_{\rm Local}$, where $\gamma_\mu/2\pi=13.5$ MHz/kG. The static field muon asymmetry signal is thus proportional to the frequency Fourier cosine transform of the local field distribution.

For a dense local-field distribution, a static muon asymmetry spectrum relaxes by the interference of infinitely many frequency components. The relaxation envelope of the oscillating signal reveals the characteristics of the field distribution. For a finite number of components, the asymmetry spectrum shows characteristic beats and (in theory) oscillates forever. For the intermediate case of several broad frequency peaks that are separated by more than their width, the muon asymmetry signal will appear ''multicomponent,'' manifesting beats, but will not recover its full amplitude in the long-time limit.

A fairly general phenomenological form for the asymmetry signal is therefore

$$A(t)=A_\perp\sum_{i\neq 0}^{I_{Max}} W_i\cos(2\pi\nu_i t)\times\exp[-(\Lambda_i t)^{\beta_{\perp i}}]$$
$$+A_\parallel\times\exp[-(\Lambda_0 t)^{\beta_\parallel}].$$

The ratios $W_i:W_j$; $i,j\neq 0$ denote the relative weights of the frequency components that are separated by more than their distribution widths, and ν_i is the mean frequency of each component. Ideally, one would also expect a variety of longitudinal relaxation signals, each characterized by its own relaxation rate Λ and exponent β, but the absence of a distinguishing frequency makes the $A_\parallel$ signal difficult to analyze in this way.

The ratio $A_\perp:A_\parallel$ (the ratio of oscillating to nonoscillating parts of the asymmetry signal) reveals the average degree to which $\hat{P}_\mu$ aligns with $\vec{B}_{\rm Local}$. Muons with $\hat{P}_\mu \| \vec{B}_{\rm Local}$ do not precess, although their polarizations may be dynamically relaxed by perpendicular fluctuations. In a homogeneous polycrystalline sample, with a static component to the local field, because the crystallites orient randomly with respect to $\hat{P}_\mu$, $A_\perp/(A_\perp+A_\|)=\frac{2}{3}$, the isotropic average perpendicular component of the muon spin. For a ceramic sample where only a $V_{\rm Ord}$ portion of the total volume $V_{\rm Tot}$ orders, $A_\perp/(A_\perp+A_\|)=\frac{2}{3}\times V_{\rm Ord}/V_{\rm Tot}<\frac{2}{3}$. In a single crystal, given $\hat{P}_\mu$, the $A_\perp$ fraction will be given by $V_{\rm Ord}/V_{\rm Tot} \times\langle\sin^2\theta_{\mu-B}\rangle$, where $\theta_{\mu-B}$ is the angle between $\hat{P}_\mu$ and $\vec{B}_{\rm local}$ at the muon site, and the brackets denote an average over domains of $V_{\rm Ord}$.

The parameters Λ and β incorporate relaxation due to the width of each component distribution and dynamics. Let Δ represent the instantaneous value of $B_{\rm local}$. When $\Lambda<\gamma_\mu\Delta$, one may distinguish dynamic from static relaxation by inspection. The relaxation of the $A_\|$ part of the asymmetry signal results from fluctuations in the perpendicular directions. Hence in a homogeneously ordered powder sample with fluctuating fields, the $A_\|=\frac{1}{3}$ fraction relaxes to zero. In such systems, there will be dynamic broadening of the oscillating components as well. A static magnetic environment, by contrast, may cause a static disorder-induced broadening of the oscillating components, but the $A_\|$ fraction persists in the long-time limit described by $t\geqslant 1/\gamma_\mu\Delta$.

However, ''the long-time limit'' may not always be accessible in the experiment. Typical time-differential μSR spectra are limited to about 10 μs. A more definitive way to distinguish dynamic relaxation from static relaxation is the application of a longitudinal field (LF) that is a few times larger than any ordered field in the sample. The muons precess about the total field with frequency ν. In sufficiently strong LF, the asymmetry does not oscillate because the local field and the initial muon polarization are nearly parallel, so that $A_\perp\rightarrow 0$. Then, any relaxation is due to dynamics that cause transitions between the local muon Zeeman states. We consider a Markovian spin decay, with an inverse spin lifetime of ν_d. When ν_d is large compared to ν, the relaxation rate probes the spectral density of the field fluctuations at energies $2h\nu$. The resulting muon asymmetry spectrum is approximately exponential in shape:

$$A(t)=A(0)\exp(-\Lambda_{\rm homog}t),$$

with

$$\Lambda_{\rm homog}=\frac{2\Delta^2\nu_d}{(2\pi\nu)^2+\nu_d^2}.$$

If the distributions of Δ or ν_d vary over the sample volume, then a modified exponential relaxation

$$A(t)=A(0)\exp[-(\Lambda t)^\beta]$$

often describes the data, where now

$$\Lambda=D\times\Lambda_{\rm homog},$$

with D, a number of order unity, and β determined by the distributions of Δ and ν_d.[26–28]

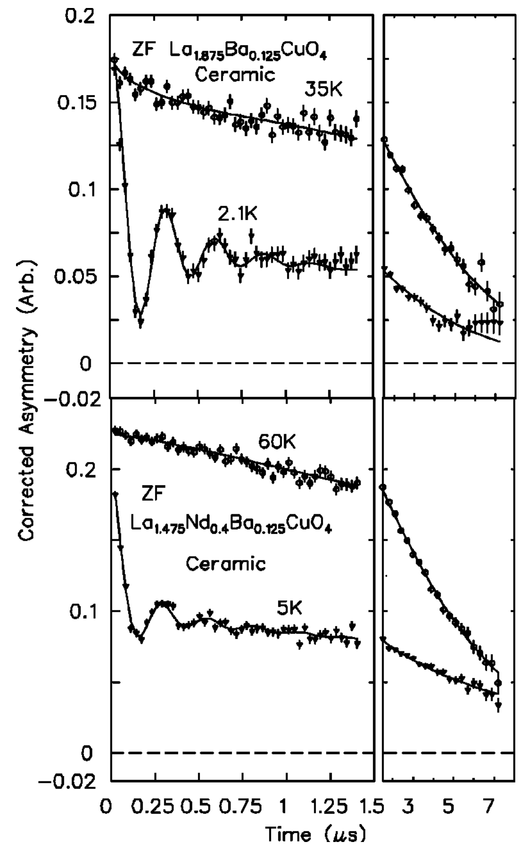

FIG. 4. Representative asymmetry spectra and fits (solid curves) for ceramic samples of $La_{1.875}Ba_{0.125}CuO_4$ and $La_{1.475}Nd_{0.4}Ba_{0.125}CuO_4$.

III. ZF-μSR TIME SPECTRA

We measured time-differential ZF-μSR spectra at the M13 and M15 surface muon channels of TRIUMF, in Vancouver, Canada. The samples were mounted in the tail of a standard Janis gas-flow cryostat with a minimum temperature of 3.5 K, or a cold-finger continuous-flow cryostat with a minimum temperature of 1.8 K. The samples were mounted on pure Ag backings. Once the stray fields at the samples were minimized, muons landing in the backings or in the (also Ag) cryostat tails did not precess noticeably over the time range studied. Because the samples under study did possess a significant nuclear magnetic moment, we are able to distinguish those muons that land in the sample even in the absence of electronic magnetic order. However, because in some setups the decay positrons due to muons landing in the Ag backing were not excluded from the histograms, the overall corrected asymmetry due to the sample alone had an arbitrary amplitude, which depended on the overall sample size with respect to the beam spot.

A. Ba- and Nd,Ba-doped samples

The ceramic $La_{1.875}Ba_{0.125}CuO_4$ samples showed spontaneous precession below $T_N\approx 30$ K, indicating magnetic order of the Cu spins. The ceramic $La_{1.475}Nd_{0.4}Ba_{0.125}CuO_4$ showed similar magnetic order with the same T_N. Figure 4 shows typical spectra from samples of each type. The spectra from both Ba-doped systems show a damped oscillation and a relaxing $A_\|$ component. It seems highly likely from Fig. 4

that substituting Nd at the La site in $La_{1.875}Ba_{0.125}CuO_4$ does not significantly affect the Cu order.

The solid curves in Fig. 4 are fits to the phenomenological form

$$A(t)=A_{\perp}\times J_0(2\pi\nu t)\times\exp(-\Lambda_{\perp}t^{\beta_{\perp}})+A_{\parallel}\times\exp(-\Lambda_{\parallel}t^{\beta_{\parallel}}).$$

Here J_0 is the zeroth-order Bessel function of the first kind. Some of the $La_{1.875}Ba_{0.125}CuO_4$ data had been fit previously with a damped cosine function.[2,4] The cosine fits tended to yield values of the initial phase of the muon asymmetry that were inconsistent with the known initial polarization of the muon beam. Some possible implications of the Bessel form for the asymmetry function are discussed below. The value of the extracted frequency does not depend strongly on which of the two functions (Bessel or cosine) is used, because the first few zeros of the functions have the same spacing to within 1%. The observed $\nu\approx 3.5$ MHz corresponds to an average $B_{local}\approx 220$ G at the muon site.

B. Ba+Sr-doped samples

Ceramic samples of $La_{1.875}Ba_{0.1}Sr_{0.025}CuO_4$ and $La_{1.875}Ba_{0.06}Sr_{0.0625}CuO_4$ showed two distinct magnetic volumes. Below 30 K, and down to 5 K, part of these samples showed a magnetic order with the same frequency as in the single-dopant samples, while the rest of the sample relaxed with the slow Kubo-Toyabe function typical to systems of small disordered moments. Similar instances of distinct magnetic regions in mixed-dopant ceramic samples have been reported previously by Lappas *et al.*,[24] who attributed the reduced ordered fraction to the decreased pinning of the stripe order as less of the lattice undergoes the LTO→LTT transition.

C. Nd,Sr-doped samples

Figure 5 shows representative spectra from crystal samples of $La_{1.475}Nd_{0.4}Sr_{0.125}CuO_4$ and $La_{1.45}Nd_{0.4}Sr_{0.15}CuO_4$. We also measured several ceramic samples at the $x=0.125$ composition that showed the same general behavior as the crystal. For $x=0.125$, T_N and ν at $5\ K<T<10$ K are nearly identical to those seen in the Ba-doped samples. For $x=0.15$, T_N is slightly lower, but the saturating ν remains unchanged. There were two significant differences between the Sr-doped and Ba-doped samples. At $T<5$ K, both ν and $\Lambda_{\perp}$ began to increase dramatically. The 3.5 K spectrum for the $x=0.15$ sample in Fig. 5 shows this effect.

As Fig. 6 shows, the LF=2 kG measurements of $La_{1.475}Nd_{0.4}Sr_{0.125}CuO_4$ crystal reveal dynamic relaxation that is almost completely absent from the $La_{1.875}Ba_{0.125}CuO_4$ ceramic.

The neutron-scattering analysis suggests that, at $T\approx 5$ K, the Nd ions begin to order following the Cu order, while the Cu moments themselves begin to cant out of the plane. We suspect that the low-temperature enhancement of the frequency may be due to the canting Cu moments, while the increased relaxation may be due to the fluctuating Nd spins. Because the Nd spins are only randomly present in the lattice, the Nd ordering should increase the relaxation rate, but should not produce any coherent oscillations. Figure 7 shows

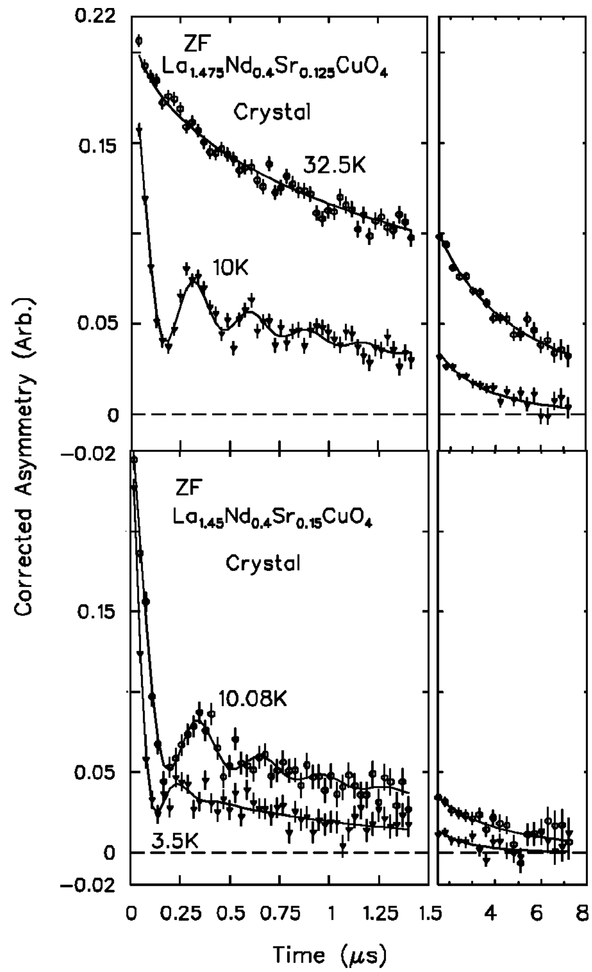

FIG. 5. Representative asymmetry spectra and fits (solid curves) for crystals of $La_{1.475}Nd_{0.4}Sr_{0.125}CuO_4$ and $La_{1.45}Nd_{0.4}Sr_{0.15}CuO_4$.

the relaxation parameters Λ and β for the $La_{1.475}Nd_{0.4}Sr_{0.125}CuO_4$ crystal, as functions of temperature. Λ increases below 5 K, suggesting that the temperature scale for the moments producing the relaxation differs markedly from T_N. β decreases to 0.45 at low temperatures, suggesting that the fluctuating magnetic field is inhomogeneous. This is consistent with the random placement of the Nd ions.

Ideally, one would like to know the direction of the magnetic field at the muon site, in order to compare it to what comes from the hypothesized spin structure. Figure 8 shows the relative oscillating volume fraction $A_{\perp}/A_{Tot}$, for ceramic and crystal samples of $La_{1.6}Nd_{0.4}Sr_{0.125}CuO_4$, which gives the value $V_{\rm Ord}/V_{\rm Tot}\times\langle\sin^2\theta_{\mu-B}\rangle$ at the muon site in the sample. The ceramic asymmetry ratio saturates at $T=10$ K. *If* that the crystal also achieves its maximal ordered volume fraction at the same temperature, then the difference in the temperature dependences of $A_{\perp}/A_{\rm Tot}$ below 10 K suggests that the Cu moments may be changing direction in this system.

D. Summary of measurements on the $x\leqslant 0.15$ samples

Figure 9 shows ν as a function of temperature for the various samples with $x\leqslant 0.15$. T_N for all of these samples is approximately the same regardless of the presence of Nd or whether the sample is doped with Ba, Sr, or both. Exclusive

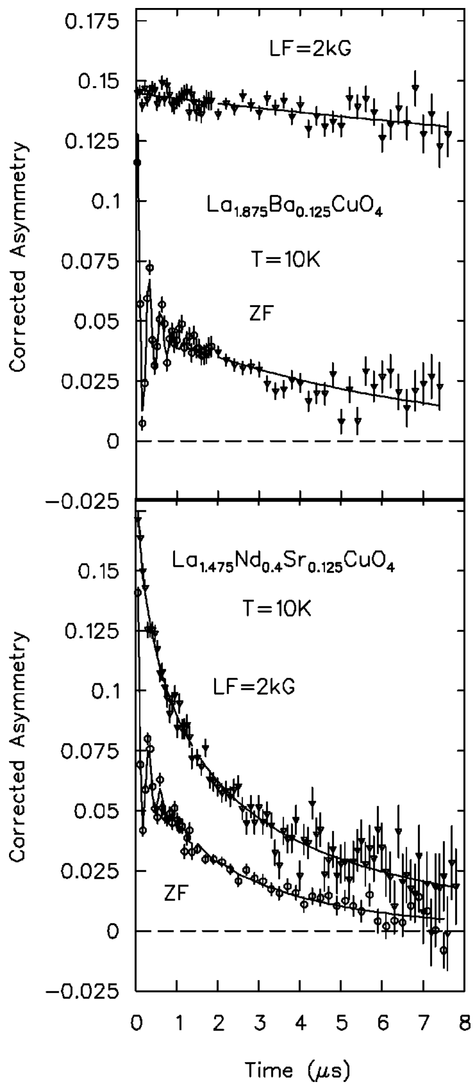

FIG. 6. Comparative decoupling at $T=10$ K and LF=2 kG for (top) Ba-doped ceramic and (bottom) Sr-doped crystal.

of the $T<5$ K enhancement in the samples with Nd, ν saturates at the same value of 3.5 MHz. This frequency results from the ordered Cu moment. Ignoring the low-temperature effects of the Nd-Cu coupling, we identify this frequency as the intrinsic magnetization of the Cu ordering in these systems. We may roughly estimate the size of the ordered moment by assuming that the muon site is unchanged from that in undoped La_2CuO_4. In this case, the ratio of the ordered moment sizes should approximately equal the ratio of the frequencies. For La_2CuO_4, Uemura *et al.* found $\nu \rightarrow 5.8$ MHz at low temperatures, for an ordered moment of approximately $0.5\mu_B$. Therefore by this method, $S_0 \approx 0.3\mu_B$. The more detailed calculation presented in the discussion below, which takes into account the modulated antiphase spin structure seen in $La_{1.475}Nd_{0.4}Sr_{0.125}CuO_4$ and $La_{1.45}Nd_{0.4}Sr_{0.15}CuO_4$,[10] gives nearly the same result.

E. $x=0.2$ samples

In contrast with the results mentioned above, ZF-μSR measurements on the $La_{1.4}Nd_{0.4}Sr_{0.2}CuO_4$ crystal revealed no coherent magnetic order for temperatures down to 1.88 K.

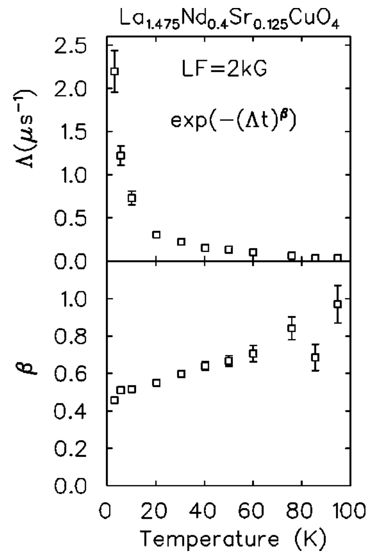

FIG. 7. Temperature dependences of (top) relaxation power Λ and (bottom) relaxation exponent β for the $La_{1.475}Nd_{0.4}Sr_{0.125}CuO_4$ crystal.

The low-temperature μSR spectrum, shown in Fig. 10, shows no static recovery, which implies that the magnetic fields in this sample remained dynamic down to 1.88 K. The initial relaxation is four times as fast as the frequency due to the ordered Cu moments in the $x=0.125$ and $x=0.15$ samples. LF measurements on a ceramic sample of the same composition show that the fast relaxation begins to decouple at 1 kG. It therefore seems likely that this fast relaxation is due to the combined quasistatic ordering of Nd and Cu moments, and that in the $x=0.20$ samples, in contrast to the lower-doping samples, the temperature scales of the Cu and Nd spin systems are not well separated. These results suggest that the magnetic order inferred from the neutron scattering data for the $x=0.20$ system[10] is in fact only quasistatic.

IV. DISCUSSION OF THE MAGNETIC ORDER

Because of the similarities among the data from all of the samples with $x=0.125$ and $x=0.15$, we analyze the mag-

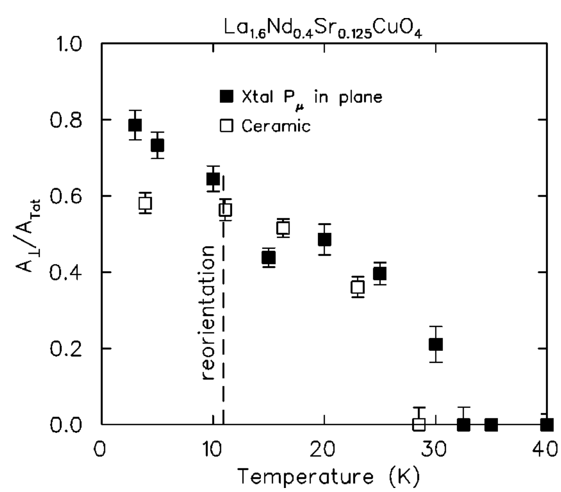

FIG. 8. Comparison of the temperature dependence of the $A_\perp/A_{Tot}$ asymmetry fraction between ceramic and crystal samples of $La_{1.475}Nd_{0.4}Sr_{0.125}CuO_4$. This quantity is proportional to $V_{\rm Ord}/V_{\rm Tot}\times\langle\sin^2\theta_{mu-B}\rangle$ at the muon site.

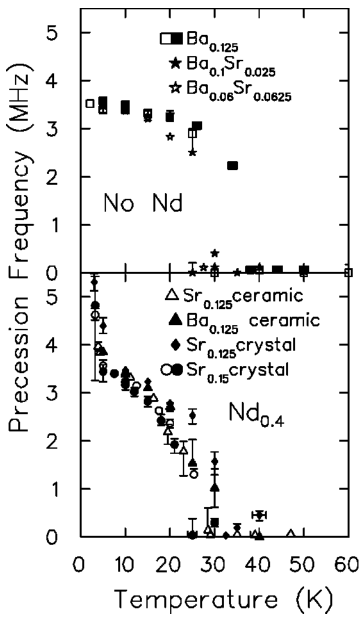

FIG. 9. Temperature dependence of the Bessel frequency extracted from fits.

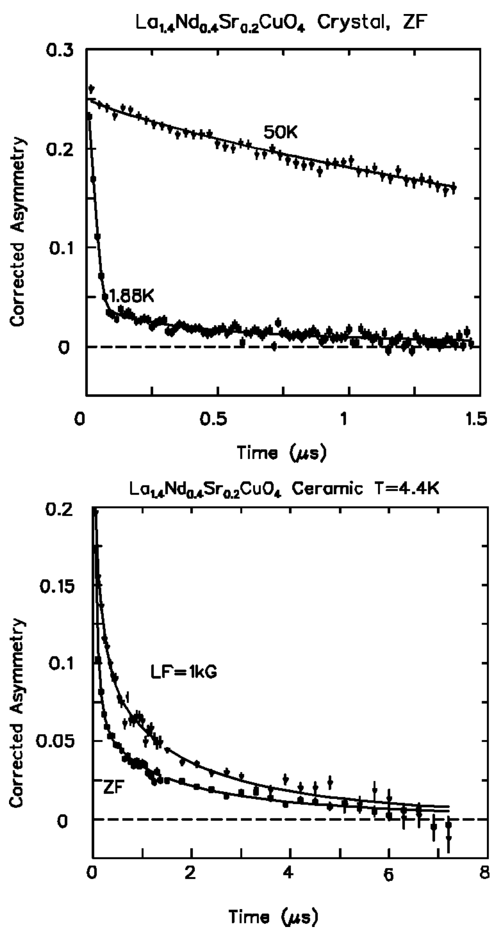

FIG. 10. ZF spectra of the $La_{1.4}Nd_{0.4}Sr_{0.2}CuO_4$ single crystal at 1.88 K, and the decoupling in 1 kG for a ceramic sample at 4.4 K.

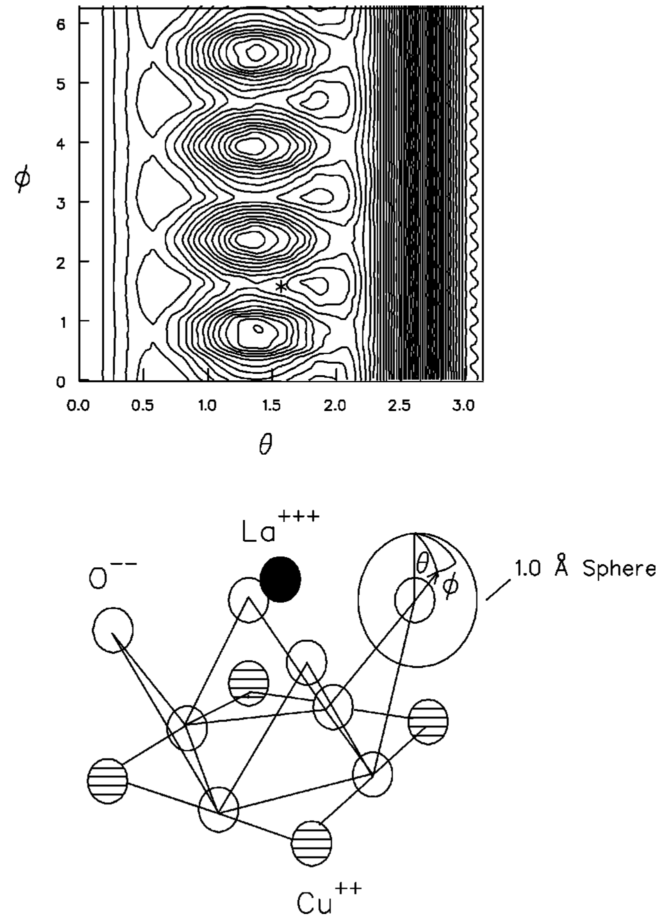

FIG. 11. The electrostatic potential energy surface as a function of θ and ϕ at a radius of 1 Å from the apical oxygen, as calculated with an Ewald sum. The asterisk denotes one of the four equivalent sites found by Hitti et al. (Ref. 22).

netic order in the same generic picture of antiphase stripe magnetic order with little correlation between different CuO_2 planes. It is important to note, however, that there is as yet no other experimental evidence for such stripe magnetism in the $La_{1.875}Ba_{0.125}CuO_4$ system. Large single crystal samples appropriate for neutron-scattering measurements have not been available. This is unfortunate, because only the $La_{1.875}Ba_{0.125}CuO_4$ system is free of the broadening due to the Nd dynamics; nevertheless, we proceed on the assumption that the two examples of magnetic order are of similar origin.

A. The muon site

To definitively extract S_0 from the measured ZF-μSR signal, we need to establish the muon site. Hitti *et al.* have deduced the muon site in undoped La_2CuO_4 by assuming that the muon resides 1.0 Å away from an oxygen site and simulating the μSR frequency as a function of the muon position in the ordered state, with the ordered moment determined by neutron scattering. They concluded that in this material the muon resides near the apical oxygen, at fractional coordinates $(x/a,y/b,z/c)=(0.253,0,0.162)$, or at an angular position ($\theta=1.569$, $\phi=n\pi/2$) on the sphere of radius 1.0 Å surrounding the apical oxygen. The barriers between these sites are due mostly to the four La ions located at the intermediate angles. This site is not the global electrostatic minimum on the spherical surface surrounding the apical oxygen.

Figure 11 shows the results of a simple Ewald calculation, assuming ionic charges, for this surface. The global minimum for undoped La_2CuO_4 occurs at $\theta = 0.66$, and a similar local minimum occurs at $\theta = 1.88$. The curvature of the potential near the minima $k \sim 0.1$ eV/Å^2. Taking the muon mass at 106 MeV, the harmonic approximation then gives a ground-state dispersion in position of $\Delta x \sim 0.4$ Å, so the muon might be localized near the local minimum of $\theta = 1.88$ in the absence of other effects such as self-trapping.

We have performed a similar Ewald calculation for the doped lattice using the average ionic charges, with essentially the same result for the potential surface. We estimated the effect of doping in the unit cell, by treating the case of Sr substitution at the La sites as an additional negative charge at one of the five La sites nearest the apical oxygen. For the most common arrangement with the substitution at one of the fourfold coordinated La sites, this had the effect of eliminating the barrier at $(2n+1)\pi/4$ on the sphere between adjacent muon sites. However, allowing the muon to reside between two minima did not introduce very different frequencies.

One mechanism that would introduce different frequencies would be to allow the muon site to become correlated with the charge modulation—if the charge modulation is made sufficiently narrow so that the muon could lower its energy by moving toward the high-spin, low-charge Cu^{++} region. However, simulations of the muon asymmetry signal, such as those described in the next section, show that this mechanism would lead to the presence of a relatively high-frequency part of the oscillating asymmetry signal, where only one frequency is observed. We therefore expect that the muon site in the doped compounds is nearly the same as that in the undoped La_2CuO_4.

B. Spin structure and simulations

μSR is a real-space probe. As such it is difficult to distinguish, using μSR, among the various possible shapes for the spin modulation. However, simulating the μSR signal allows us to confirm that (1) the dominant frequency of the μSR signal is fairly independent of the shape of the modulation, and that (2) the presence of the antiphase stripe order does not significantly alter the simple frequency-ratio calculation of S_0.

Our simulations assembled the antiphase modulated spin lattice several times with the phase of the modulation in each plane randomly assigned to one of the values allowed by the commensurate modulation length (for a commensurate modulation) or to any value (for an incommensurate modulation). The magnetic field at the muon site was then calculated assuming a dipolar magnetic coupling between the electron spins and the muon spin.

The results for three different static modulations with $S_0 = 1\mu_B$ are shown in Fig. 12. The characteristics of each may be understood simply as the result of the differing local spin structures near the muon site. For the simple sinusoidal modulation with wavelength of 8 lattice units, three different spin sizes $(1,1/\sqrt{2},0)$ lead to three frequency peaks. For the blocked-sinusoidal modulation of the same wavelength, two spin sizes lead to two peaks; and for an incommensurate modulation there is a continuum of allowed spin sizes and muon precession frequencies. A fourth kind of modulation, related to the incommensurate spectrum, involves disordered pinnings of the stripes which gives a locally incommensurate modulation with a variable wavelength. Intraplanar phase disorder (as distinguished from incommensurability) could result from inhomogeneous pinning of intrinsically commensurate stripes which stretches out the fundamental modulation and thereby introduces a continuum of local spin sizes. The effects of phase disorder and incommensurability would be indistinguishable in μSR measurements.

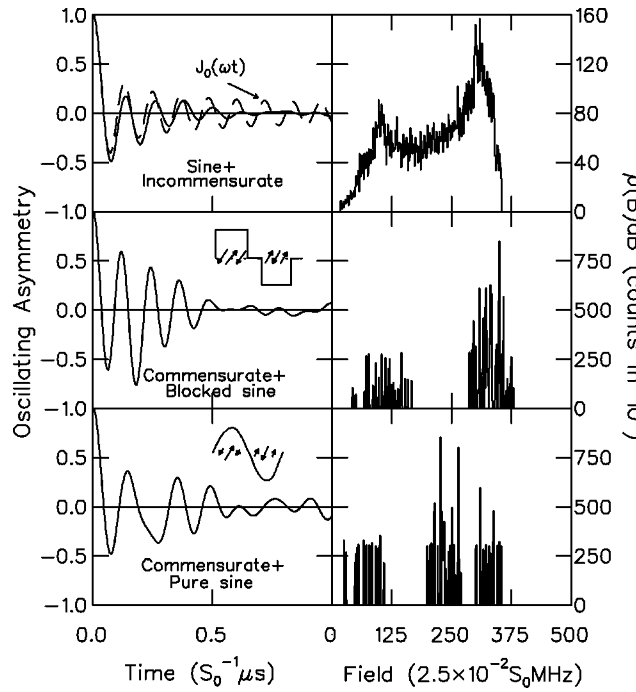

FIG. 12. Simulated $A_\perp$ component of the muon asymmetry spectrum for various shapes of the spin modulation, along with the corresponding magnetic-field distributions at the muon site.

The shape of the spin modulation envelope in the $La_{1.475}Nd_{0.4}Sr_{0.125}CuO_4$ system has been determined by neutron scattering to be primarily sinusoidal. Bragg peaks from the higher harmonics would only have been a few percent of the intensity due to the (already small) fundamental reflection. The simulations from each of the modulations discussed above may be made to resemble the observed spectrum for $La_{1.875}Ba_{0.125}CuO_4$ by including appropriate amounts of Gaussian disorder or phase disorder/incommensurability. The simplest scenario consistent with both the μSR and neutron scattering results is a sinusoidal modulation with a high degree of incommensurability or phase disorder.

According to the results of Fig. 12, the fundamental frequency observed for each of these spin structures would be approximately the same. Scaling the frequency for the incommensurate modulation simulation to the measured frequency in $La_{1.875}Ba_{0.125}CuO_4$ gives $S_0 \approx 0.34\mu_B$ for this spin structure.

C. Comparison with neutron-scattering measurements

S_0 from the neutron scattering measurements[11] $\approx 0.1\mu_B$, which is a factor of 3 smaller than S_0 derived from μSR. A likely explanation for this disparity is that, since neutron

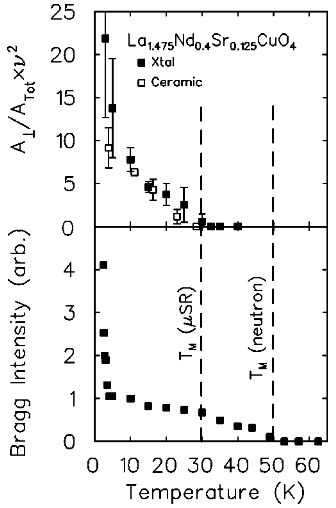

FIG. 13. Comparison of neutron scattering magnetic Bragg intensity of the satellite peak in $La_{1.475}Nd_{0.4}Sr_{0.125}CuO_4$ to the analogous quantity derived from the μSR measurements.

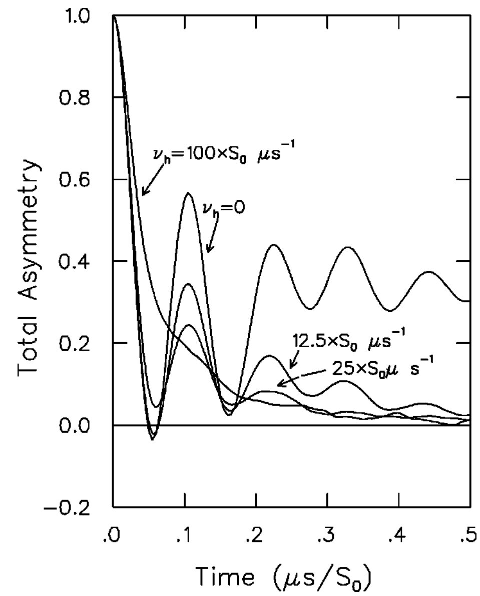

FIG. 14. The effect of stripe motion of the Gaussian-broadened spectrum for the blocked-sine modulation.

scattering is a nonlocal probe, disorder in the direction and phase of the magnetic modulation reduce S_0(neutron) as compared to $S_0(\mu\mathrm{SR})$. A similar effect has been inferred from the comparison of μSR and neutron-scattering measurements of S_0 for the low-T_N samples of La_2CuO_{4-y}.[20]

The measured values of T_N also substantially differ between the two techniques. In Fig. 13, we compare the scaled intensity of the magnetic Bragg peak along with the analogous quantity derived from the μSR data, $A_\perp|\nu|^2$. The μSR and neutron-scattering data for the crystal were taken on the same sample. In the neutron-scattering experiment, the charge-ordering peaks show finite intensity below $T_{CO}\approx 60$ K, and the magnetic peaks show finite intensity below $T_N\approx 50$ K. However, as noted above, the μSR measurements show no magnetic order until the temperature drops below 30 K. The cause of this disagreement may be the coarser energy resolution of the neutron-scattering experiment. Indeed, neutron-scattering measurements of different crystals of $La_{1.475}Nd_{0.4}Sr_{0.125}CuO_4$ with tighter energy resolutions show that the magnetic Bragg peak of the spin modulation broadens substantially above $T_N(\mu\mathrm{SR})$.[29] This implies that the magnetism between T_N(neutrons) and $T_N(\mu\mathrm{SR})$, is only quasistatic, with true static order below $T_N(\mu\mathrm{SR})$. These results are also consistent with the evidence that the magnetism seen in the $x=0.20$ system is quasistatic. In the $x=0.125$ system, apparently, the pinning effect is more pronounced.

We have simulated the effect of slow fluctuations of the spin stripe positions on the static $La_{1.875}Ba_{0.125}CuO_4$ spectrum. The effect of spin fluctuations within a stripe should be similar, since for the locally nearly AF order the effect of spin flips or stripe movement beneath the muon are almost equivalent. Similarly, the effect of fluctuations within commensurate and incommensurate spin structures would be almost the same.

We compare the relaxation of the $A_\parallel$ aligned component in $La_{1.875}Ba_{0.125}CuO_4$ to the simulated relaxation rate to roughly estimate the upper limit of such a fluctuation rate. Our simulation was dynamicized as follows: for each time step, we calculated the local dipolar field at the muon site. The muon polarization was developed according to the Bloch equations for the expectation values of the spin.

Figure 14 shows the results for the blocked-sine modulation with static Gaussian broadening and $S_0=1$, with several values of the hopping probability per nanosecond ν_h. Values of ν_h down to about $12.5\times S_0\ \mu\mathrm{s}^{-1}$ would induce a relaxation of the $A_\parallel$ asymmetry component which is stronger, in relation to the oscillation frequency, than the rate seen in the data for the statically ordered $La_{1.875}Ba_{0.125}CuO_4$ ceramic samples. Hence our data confirm that the spins are static, with an upper limit for the hop rate of $\nu_h=3.75\ \mu\mathrm{s}^{-1}$ well below $T_N(\mu\mathrm{SR})$.

We now briefly discuss the support in the neutron-scattering measurements for the incommensurate or phase-disordered lineshape described by a damped Bessel function. The neutron-scattering measurements of Tranquada *et al.* on $La_{1.475}Nd_{0.4}Sr_{0.125}CuO_4$ yield an incommensurate magnetic modulation wavevector of $\epsilon\approx 0.118\times 2\pi/a$. One possible explanation for this very incommensurate value is that about 25% of the charge stripes are slightly displaced[11] from the position they would have in a commensurate modulation. The difference between $S_0(\mu\mathrm{SR})$ and S_0(neutron) implies that disorder plays a strong role in this system. ϵ of the dynamic modulations seen in SC samples increases proportionately to x. As x increases above 0.125, ϵ changes very slowly.[10] This suggests that the stripes tend to be pinned at a single spacing, even as the charge density increases. Furthermore, one might expect by this argument the gradual destruction of the static stripe phase as doping increases much beyond $x=0.125$, as is seen for $x=0.20$.

As we mentioned above, the neutron measurements also suggest that the Cu moments cant out of the plane below $T\sim 5$ K. Simulations for the incommensurate modulation suggest that the field at the muon site will be enhanced, which is consistent with the observed trend. However, as there is a tradeoff in the fitting between relaxation and oscillation in the fast-relaxing signals, more quantitative comparisons are difficult to make. For muon site given above, a uniform cant-

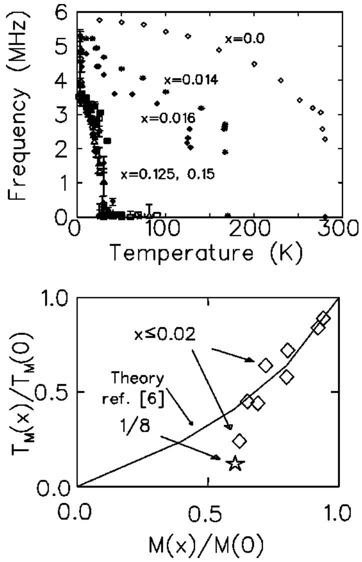

FIG. 15. Upper panel: the μSR precession frequency for lightly doped AF $La_{2-x}Sr_xCuO_4$ with $x<0.02$. The data from the present study for $x\geqslant0.125$ is also shown. Lower panel: a plot of the reduced $T_N(x)$ and $M(T=0,x)$ for lightly doped AF $La_{2-x}Sr_xCuO_4$ along with the prediction of Hone and Castro-Neto (from Ref. 6), and the data from the more highly doped samples in the present study.

ing of the Cu spins by $\pi/4$ out of the plane would tend to increase the $A_\perp/A_{\rm Tot}$ ratio for $\hat{P}_\mu$ in the CuO_2 plane. This result is in agreement with the observed trend in $La_{1.6}Nd_{0.4}Sr_{0.125}CuO_4$ which was shown in Fig. 8, but quantitative comparisons require more information on the ordered volume fraction in the $La_{1.6}Nd_{0.4}Sr_{0.125}CuO_4$ crystal.

D. Comparison to AF La_2CuO_4 systems

Figure 15 compares the μSR frequencies for the samples in this study to the frequencies in the $x<0.02$ samples measured by Borsa *et al.*[5] The doped AF samples show evidence of two transitions. At intermediate temperatures, the precession frequency in $La_{1.984}Sr_{0.016}CuO_4$ is comparable to that seen in the $x=0.125$ samples. However at $T<50$ K, there is an enhancement of the frequency in $La_{1.984}Sr_{0.016}CuO_4$ and $La_{1.986}Sr_{0.014}CuO_4$ which brings the ordered moments up to almost the full value for La_2CuO_4. Borsa *et al.* have explained the reduced magnetization in the intermediate temperature range as the result of finite size effects due to the segregation of the doped holes in the CuO_2 plane. Hone and Castro-Neto[6] have proposed an explanation of the reduction of T_N at light dopings in a similar physical picture by estimating the effect of an anisotropy in the magnetic coupling in the directions along and across the stripes. We plot the extrapolated zero-temperature magnetizations $M(x=0.125)/M(x=0)$, and $T_N(x=0.125)/T_N(0)$ along with the results of Borsa *et al.* and the finite-size theory in the lower panel Fig. 15. An important difference between the lightly doped AF and the situation in the $x\geqslant0.125$ systems is that the antiphase magnetic order in the latter allows for stronger correlations through the regions where the spin is suppressed. Hence, while real-space renormalization calculations for the lightly-doped AF show a crossover from two-dimensional domains of correlated spins to one-dimensional domains, and a concomitant loss of AF order at $x\sim0.025$, the antiphase magnetic order is more robust and should be less reduced in dimension with doping.

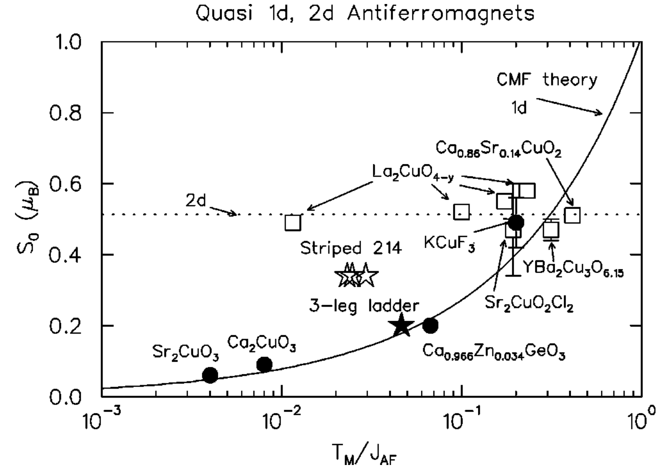

FIG. 16. A comparison of quasi-one-dimensional (closed circles) (Refs. 25 and 31), quasi-two-dimensional (open squares) (Refs. 20 and 32–34), and stripe (stars) AF systems. The solid curve is the relationship between S_0 and T_N/J_{AF} derived in Ref. 30. The dotted line roughly defines the observed S_0 in all quasi-two-dimensional systems.

E. Dimensionality of the magnetic order

Various μSR experiments highlight the importance of magnetic exchange anisotropy in determining S_0 for the various cuprate antiferromagnetic systems. The quasi-one-dimensional, chainlike systems Sr_2CuO_3, Ca_2CuO_3, $KCuF_3$, and $Ca_{0.966}Zn_{0.034}GeO_3$ have been studied by Kojima *et al.*,[25] who showed that, if one scales T_N by the stronger antiferromagnetic exchange along the chain direction (denoted J_{AF}) then S_0 decreases with T_M/J_{AF}. The behavior of all of the one-dimensional systems measured with μSR is very well described by the "chain mean-field" (CMF) theory of Affleck.[30] The CMF theory treats each chain exactly in the mean field due to the other chains.

The data for the quasi-1D systems as well as the prediction of the chain mean-field theory are reproduced in Fig. 16. To this figure we add points for the quasi-2D cuprate antiferromagnets composed of stacked CuO_2 planes: $Sr_2CuO_2Cl_2$, $Ca_{0.86}Sr_{0.14}CuO_2$, $YBa_2Cu_3O_{6.15}$, and La_2CuO_{4-y} systems.[20,31–34] These quasi-2D systems all have $S_0\approx0.5\mu_B$, independent of T_N.

We now place the striped systems into this context. Let us assume that the coupling within the stripes does not change very much from the case of La_2CuO_4. Then, using a nominal value of $J_{AF}\approx1300$ K, we find that the striped systems intermediate between the quasi-1D and quasi-2D limits. For another comparison, we also plot a point for the "3-leg ladder" material $Sr_4Cu_6O_{10}$.[35] As Fig. 17 shows, the structures of the stripe and ladder materials are similar in that both consist of nominally antiferromagnetic strips, three lattice constants across. For the ladder material, however, the interladder coupling is strongly frustrated. In the plot of Fig. 16, the ladder material falls in the quasi-1D regime. These com-

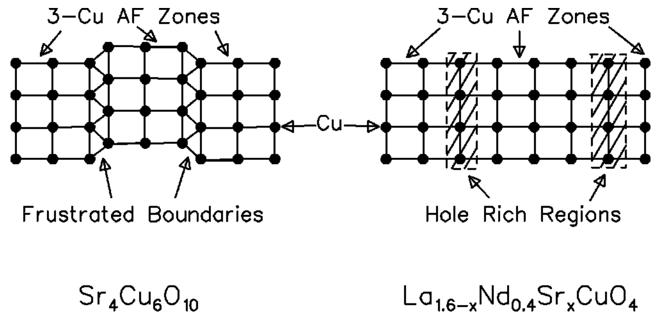

FIG. 17. A comparison of (left) the 3-leg ladder cuprate $Sr_4Cu_6O_{10}$ and (right) the CuO_2 plane with hole stripes.

parisons suggest that the couplings across the boundaries for the stripe materials are comparatively stronger than for the quasi-1D materials, and that the electronic state in the ordered stripe material is not much reduced in dimensionality from that in the undoped cuprate.

V. SUPERCONDUCTIVITY: TF-μSR MEASUREMENTS ON $x=0.15$, $x=0.20$ SAMPLES

Emery, Kivelson, and Zachar,[36] and Castro-Neto and Hone,[37] have developed theories of superconductivity involving coherent arrays or networks of charge stripes in an antiferromagnetic background. Here we present TF-μSR hysteresis measurements that are consistent with the existence of microscopic superconducting networks even in the magnetically ordered state.

In TF μSR, muons are implanted into the sample with their spins initially perpendicular to an applied magnetic field $\vec{H}$. In the absence of any local inhomogeneities in the magnetic field, the muons would precess coherently, and the asymmetry function would be

$$A(t)=A(0)\cos(2\pi\nu t+\phi),$$

where $\nu=\gamma_\mu/2\pi H$, and ϕ corresponds to the initial direction of the muon spin. As in the ZF case, static and dynamic local fields broaden the frequency distribution and lead to a relaxation of the homogeneous field signal. In this case,

$$A(t)=A(0)\cos(2\pi\overline{\nu}t+\phi)\times G(t),$$

where $G(t)$ is a relaxation envelope and $\overline{\nu}=\gamma_\mu/2\pi\overline{B}_{\mathrm{local}}$. Here we are neglecting the effects on the frequency due to electronic polarization in the magnetic field, which is small for most systems.

There are two common ways to examine superconductivity in type-II materials with TF μSR. First, in field cooling (FC) below T_c with $H_{c1}<H<H_{c2}$, the finite penetration depth of the magnetic field will broaden the static field distribution. In many cases this allows one to estimate the penetration depth from the static TF muon relaxation function. Unfortunately, in the systems considered here, the large dynamic relaxation due to the Nd moments makes an extraction of the static broadening difficult. Therefore, to test whether the samples containing Nd were superconductors, we compared the FC and zero-field-cooled (ZFC) TF relaxation rates. Below the flux-pinning temperature T_p in a superconductor, these two rates should diverge with the ZFC rate becoming larger due to inhomogeneous pinning in the flux lattice. The $La_{1.45}Nd_{0.4}Sr_{0.15}CuO_4$ and $La_{1.4}Nd_{0.4}Sr_{0.2}CuO_4$ crystals were mounted on silver backing, behind a silver mask in a cold-finger cryostat. The asymmetries from the sample and the mask were counted separately, in a specialized Knight-shift apparatus.[38] The degree of relaxation from the silver mask signal provided a rough check of the strength of the fringing fields in the sample.

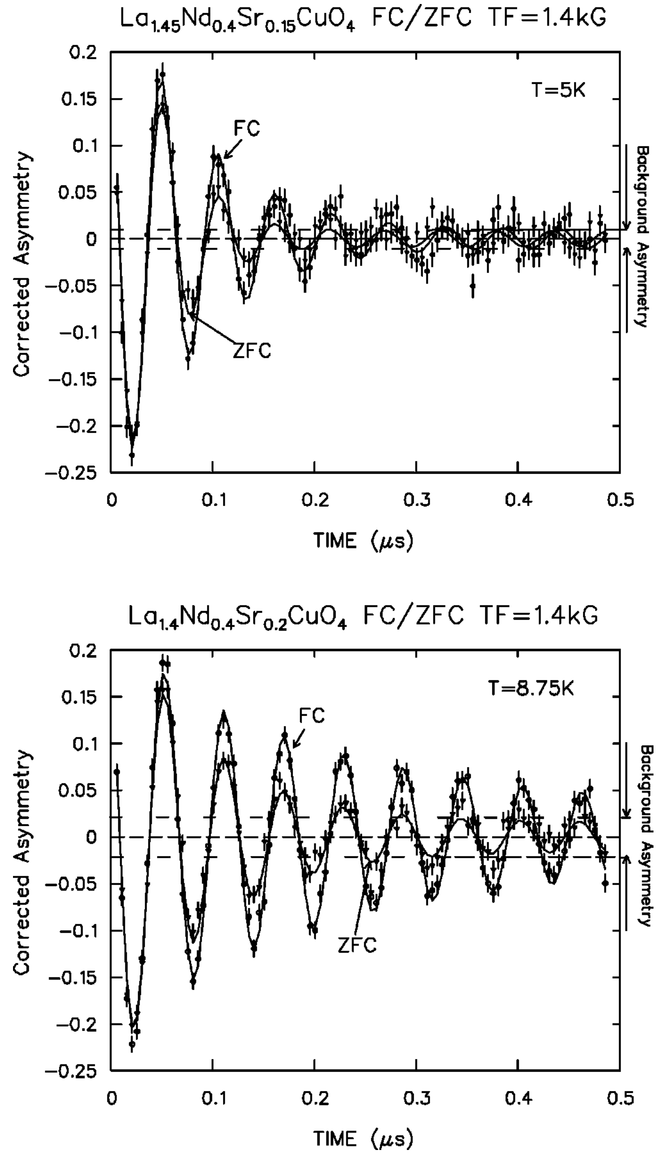

FIG. 18. Comparison of FC and ZFC asymmetry spectra below T_p for an applied TF of 1400 G.

The relaxation envelope in the sample signal was fit to the form $G(t)=\exp[-(\Lambda t)^\beta]$. In addition, there was a small background signal estimated from a small long-lived component of the oscillating asymmetry, most likely due to muons from the silver backing. For both samples, the background signal accounted for less than 10% of the total asymmetry. Figure 18 compares sample spectra in FC and ZFC showing pronounced differences in relaxation rate. The comparative relaxation rates of the sample asymmetry are shown as a function of temperature in Fig. 19.

Below 7.5 K in $La_{1.45}Nd_{0.4}Sr_{0.15}CuO_4$ and 12.5 K in $La_{1.4}Nd_{0.4}Sr_{0.2}CuO_4$, there is a large difference between the

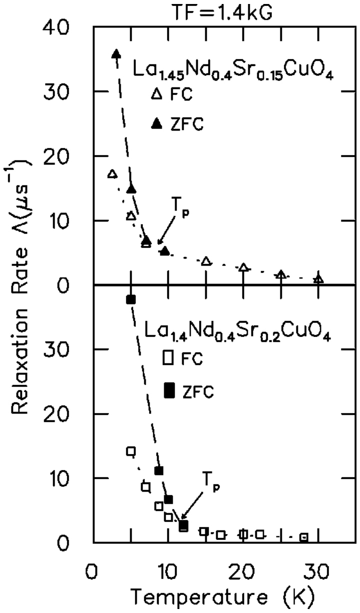

FIG. 19. The FC and ZFC TF-μSR relaxation rates in $La_{1.45}Nd_{0.4}Sr_{0.15}CuO_4$ and $La_{1.4}Nd_{0.4}Sr_{0.2}CuO_4$ crystals, in an applied field of 1400 G.

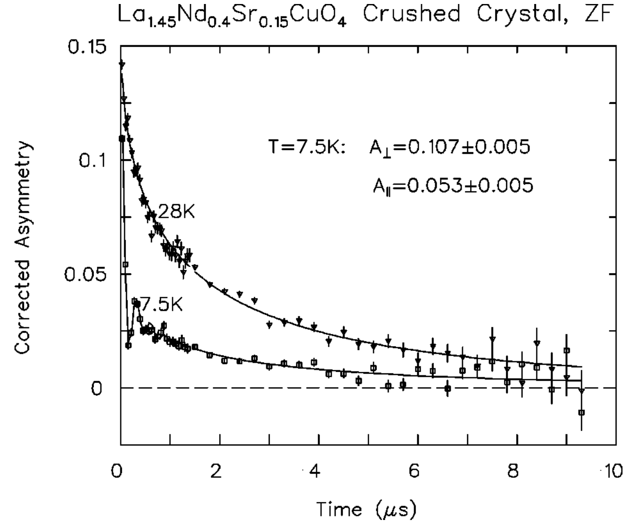

FIG. 20. ZF spectra of the pulverized single-crystal sample of $La_{1.45}Nd_{0.4}Sr_{0.15}CuO_4$.

FC and ZFC relaxation rates. The relatively large relaxation rate in $La_{1.45}Nd_{0.4}Sr_{0.15}CuO_4$ for $T_p<T<20$ K suggests that in this temperature regime, the static magnetic field is broadened due to the magnetic order in this system. Clearly, the relaxation rate is enhanced for the entire asymmetry in each sample. The T_p value for $La_{1.45}Nd_{0.4}Sr_{0.15}CuO_4$ is roughly consistent with the SQUID measurements of Ostenson *et al.*, who found an irreversibility field of 4.5 kG at $T=6$ K (Ref. 18) in a different sample of this material.

These TF-μSR measurements by themselves do not rule out the possibility of patchy superconductivity on the scale of the London penetration depth. The effect of the fringe fields in the vortex state in ZFC is so large that the case of a disordered flux expulsion into nonsuperconducting patches of the sample could be largely indistinguishable from the case of uniform superconductivity with a disordered flux lattice. Indeed, in ZFC, the asymmetry from the silver mask was strongly relaxed, while in FC this relaxation was negligible. However, the large hysteresis effect suggests that in these materials, superconductivity and magnetism coexist in the same regions of the sample. We checked this explicitly for the $La_{1.45}Nd_{0.4}Sr_{0.15}CuO_4$ by pulverizing the same crystal used in the hysteresis measurements.

The ZF-μSR spectra in Fig. 20 show that magnetic order with $A_\perp/A_\parallel=2.02\pm0.21$ occurred *in the same sample*. Because of the Nd moments throughout the sample, there will be no regions of the sample where the μSR asymmetry does not relax. Hence the presence of a volume fraction that is invisible in ZF is highly unlikely. We may therefore estimate the upper limit of any unordered volume fraction from the lower limit of the observed $A_\perp:A_\parallel$ ratio. Calling the unordered part of the total asymmetry δ, we have

$$\frac{\frac{2}{3}(A_{tot}-\delta)}{\frac{1}{3}(A_{tot}-\delta)+\delta}=\frac{A_\perp}{A_\parallel}.$$

Then,

$$\frac{\delta}{A_{tot}}=\frac{2-A_\perp/A_\parallel}{2+A_\perp/A_\parallel}.$$

Plugging in the numbers gives $\delta/A_{tot}\approx0.035$, which means that virtually the entire sample, with a lower limit of $\approx$97% of the volume, was in the magnetically ordered state.

VI. SUMMARY

We have presented the ZF-μSR spectra in several 214 cuprate systems where superconductivity has been suppressed in concert with the LTO→LTT transition. The data from all samples are best described by a modulation that yields a single frequency within the uncertainties of the asymmetry spectrum. On the time scale of μSR, the order is describable as an incommensurate static modulation of antiferromagnetic order, or a commensurate modulation with large inhomogeneous pinning effects. In the $La_{1.875}Bs_{0.125}CuO_4$ system, at the least, the magnetism is static to within a small fraction of the spontaneous precession frequency.

There is strong evidence, from the successful neutron-scattering analysis of the Nd low-temperature interplanar correlations, and the LF-μSR data presented here, that in $La_{1.6-x}Nd_{0.4}Sr_xCuO_4$, for $x=0.125$ and $x=0.15$, the Nd and Cu spin systems remain distinct down to $T\approx5$ K.

The size of the ordered Cu moment, S_0, at 10 K is constant within the uncertainties for all of the samples showing spontaneous precession, with a value estimated at $0.3\mu_B$. Simple comparisons of S_0 and the T_N/J_{AF} ratio to those for quasi-1D and quasi-2D spin-1/2 cuprate antiferromagnets suggest that the magnetic order in the stripe systems may be close to the two-dimensional limit.

Measurements of the TF relaxation rates in single crystal $La_{1.45}Nd_{0.4}Sr_{0.15}CuO_4$ and $La_{1.4}Nd_{0.4}Sr_{0.2}CuO_4$ samples suggest that, in addition to the bulk magnetic transition, these samples also become superconducting below 10 and 7 K, respectively. ZF-μSR measurements on the pulverized crystal of $La_{1.45}Nd_{0.4}Sr_{0.15}CuO_4$ show that the entire volume of this sample is entirely magnetically ordered. This observation suggests that superconductivity and magnetic order coexist in the same volume of this material.

ACKNOWLEDGMENTS

We gratefully acknowledge the insights of John Tranquada. We also thank Syd Krietzman, Bassam Hitti, Donald Arseneau, Mel Good, and Curtis Ballard (all at TRIUMF) for valuable technical support. The work at Columbia was funded under a NEDO International Joint Research grant, and NSF Grant Nos. DMR-95-10453 and DMR-95-10454. Work at LANL was performed under the auspices of the DOE. Work at U. C. Riverside was supported by NSF Grant No. DMR-94-18991.

---

*Present address: Technion, Haifa 32000, Israel.

†Present address: Department of Superconductivity, University of Tokyo, Bunkyo-ku, Tokyo, Japan.

[1] J. D. Axe, A. H. Moudden, D. Hohlwein, D. E. Cox, K. M. Mohanty, and A. R. Moodenbaugh, Phys. Rev. Lett. **62**, 2751 (1989).

[2] G. M. Luke, L. P. Le, B. J. Sternlieb, W. D. Wu, Y. J. Uemura, J. H. Brewer, T. M. Riseman, S. Ishibashi, and S. Uchida, Physica C **185–9**, 185 (1991).

[3] K. Kumagai, K. Kawano, I. Watanabe, K. Nishiyama, and K. Nagamine, Hyperfine Interact. **86**, 473 (1994).

[4] G. M. Luke, K. Kojima, M. Larkin, J. Merrin, B. Nachumi, Y. J. Uemura, Y. Nakamura, S. Uchida, and M. Crawford, Hyperfine Interact. **105**, 113 (1997).

[5] F. Borsa, P. Carretta, J. N. Cho, F. C. Chou, Q. Nu, D. C. Johnston, A. Lascialfari, D. R. Torgeson, R. J. Gooding, N. M. Salem, and K. J. E. Vos, Phys. Rev. B **52**, 7334 (1995).

[6] Daniel Hone and A. H. Castro Neto, cond-mat/9701042 (unpublished); A. H. Castro Neto and Daniel Hone, Phys. Rev. Lett. **76**, 2165 (1996).

[7] S-W. Cheong, G. Aeppli, T. E. Mason, H. Mook, S. M. Hayden, P. C. Canfield, Z. Fisk, K. N. Clausen, and J. L. Martinez, Phys. Rev. Lett. **67**, 1791 (1991).

[8] T. R. Thurston, P. M. Gehring, G. Shirane, R. J. Birgeneau, M. A. Kastner, Y. Endoh, M. Matsuda, K. Yamada, H. Kojima, and I. Tanaka, Phys. Rev. B **46**, 9128 (1992).

[9] T. E. Mason, G. Aeppli, S. M. Hayden, A. P. Ramirez, and H. A. Mook, Phys. Rev. Lett. **71**, 919 (1993).

[10] J. M. Tranquada, B. J. Sternlieb, J. D. Axe, Y. Nakamura, and S. Uchida, Nature (London) **375**, 561 (1995); J. M. Tranquada, J. D. Axe, N. Ichikawa, A. R. Moodenbaugh, Y. Nakamura, and S. Uchida, Phys. Rev. Lett. **78**, 338 (1997).

[11] J. M. Tranquada, J. D. Axe, N. Ichikawa, Y. Nakamura, S. Uchida, and B. Nachumi, Phys. Rev. B **54**, 7489 (1996).

[12] T. Nagano, Y. Tomioka, Y. Nakayama, K. Kishio, and K. Kitazawa, Phys. Rev. B **48**, 9689 (1993).

[13] M. K. Crawford, R. L. Harlow, E. M. McCarron, W. E. Farneth, J. D. Axe, H. Chou, and Q. Huang, Phys. Rev. B **44**, 7749 (1991).

[14] Y. Nakamura and S. Uchida, Phys. Rev. B **46**, 5841 (1992).

[15] B. Büchner, M. Breuer, A. Freimuth, and A. P. Kampf, Phys. Rev. Lett. **73**, 1841 (1994).

[16] J. M. Tranquada, D. J. Buttrey, V. Sachan, and J. E. Lorenzo, Phys. Rev. Lett. **73**, 1003 (1994).

[17] Yimei Zhu, A. R. Moodenbaugh, Z. X. Cai, J. Tafto, M. Suenaga, and D. O. Welch, Phys. Rev. Lett. **73**, 3026 (1994).

[18] J. E. Ostenson, S. Bud'ko, M. Breitwisch, D. K. Finnemore, N. Ichikawa, and S. Uchida, Phys. Rev. B **56**, 2820 (1997).

[19] Y. J. Uemura, W. J. Kossler, X. H. Yu, J. R. Kempton, H. E. Schone, D. Opie, C. E. Stronach, D. C. Johnston, M. S. Alvarez, and D. P. Goshorn, Phys. Rev. Lett. **59**, 1045 (1987).

[20] Y. J. Uemura, W. J. Kossler, J. R. Kempton, X. H. Yu, H. E. Schone, D. Opie, C. E. Stronach, J. H. Brewer, R. F. Kiefl, S. R. Kreitzman, G. M. Luke, T. Riseman, D. Ll. Williams, E. J. Ansaldo, Y. Endoh, E. Kudo, K. Yamada, D. C. Johnston, M. Alvarez, D. P. Goshorn, Y. Hidaka, M. Oda, Y. Enomoto, M. Suzuki, and T. Murakami, Physica C **153-155**, 769 (1988).

[21] D. R. Harshman, G. Aeppli, G. P. Espinosa, A. S. Cooper, J. P. Remeika, E. J. Ansaldo, T. M. Reisman, D. Ll. Williams, D. R. Noakes, B. Ellman, and T. F. Rosenbaum, Phys. Rev. B **38**, 852 (1988).

[22] B. Hitti, P. Birrer, K. Fischer, F. N. Gygax, E. Lippelt, H. Maletta, A. Schenck, and M. Weber, Hyperfine Interact. **63**, 287 (1990).

[23] W. Wagener, H.-H. Klaus, M. Hillberg, M. A. C. de Melo, M. Birke, F. J. Litterst, E. Schrier, B. Büchner, and H. Micklitz, Hyperfine Interact. **105**, 107 (1997).

[24] A. Lappas, L. Cristofolini, K. Prassides, K. Vavekis, A. Amato, F. N. Gygax, M. Pinkpank, and A. Schenck, Hyperfine Interact. **105**, 101 (1997).

[25] K. M. Kojima, Y. Fudamoto, M. Larkin, G. M. Luke, J. Merrin, B. Nachumi, Y. J. Uemura, N. Motoyama, H. Eisaki, S. Uchida, K. Yamada, Y. Endoh, S. Hosoya, B. J. Sternlieb, and G. Shirane, Phys. Rev. Lett. **78**, 1787 (1997), and references therein.

[26] A. Keren, Phys. Rev. Lett. **72**, 3254 (1994).

[27] R. S. Hayano, Y. J. Uemura, J. Imazato, N. Nishida, T. Yamazaki, and R. Kubo, Phys. Rev. B **20**, 850 (1979); K. M. Kojima, Ph.D. thesis (unpublished).

[28] R. H. Heffner, L. P. Le, M. F. Hundley, J. J. Neumeier, G. M. Luke, K. Kojima, B. Nachumi, Y. J. Uemura, D. E. MacLaughlin, and S.-W. Cheong, Phys. Rev. Lett. **77**, 1869 (1996).

[29] J. Tranquada (unpublished).

[30] Ian Affleck, J. Phys. A **27**, 7313 (1994).

[31] K. Kojima, A. Keren, G. M. Luke, B. Nachumi, W. D. Wu, Y. J. Uemura, M. Azuma, and M. Takano, Phys. Rev. Lett. **74**, 2812 (1995).

[32] D. Vaknin, S. K. Sinha, C. Stassis, L. L. Miller, and D. C. Johnston, Phys. Rev. B **41**, 1926 (1990).

[33] A. Keren, L. P. Le, G. M. Luke, B. J. Sternlieb, W. D. Wu, and Y. J. Uemura, Phys. Rev. B **48**, 12 926 (1993).

[34] S. Shamoto, M. Sato, J. M. Tranquada, B. J. Sternlieb, and G. Shirane, Phys. Rev. B **48**, 13 817 (1993).

[35] K. M. Kojima (unpublished).

[36] V. J. Emery, S. Kivelson, and O. Zachar, Phys. Rev. B **56**, 6120 (1997).

[37] A. H. Castro Neto and Daniel Hone, Phys. Rev. Lett. **76**, 2165 (1996).

[38] This apparatus was designed by S. Dunsinger at UBC.